DOI: 10.1002/eej.23267

TRANSLATED PAPER

WILEY

Economic evaluation of charging/discharging control of electric vehicles as system flexibility considering control participation rate

Nanami Yoshioka[1] | **Hiroshi Asano**[2,3] | **Shigeru Bando**[1,2,3]

[1]Socio-economic Research Center, Central Research Institute of Electric Power Industry, Chiyoda-ku, Tokyo, Japan

[2]Department of Human and Engineered Environmental Studies, Graduate School of Frontier Science, The University of Tokyo, Kashiwa, Chiba, Japan

[3]Energy Innovation Center, Central Research Institute of Electric Power Industry, Yokosuka, Kanagawa, Japan

Correspondence
Nanami Yoshioka, Socio-Rsearch Center, Central Research Institute of Electric Power Industry, 1-6-1 Otemachi, Chiyoda-ku, Tokyo 100-8126, Japan.
Email: yoshioka3765@criepi.denken.or.jp

Translated from Volume 139 Number 12, pages 713–721, DOI: 10.1541/ieejpes.139.713 of *IEEJ Transactions on Power and Energy* (Denki Gakkai Ronbunshi B)

Abstract

In Japan, installed capacity of variable renewable generation (VRG) is rapidly increasing. Through the efforts to make VRG into one of main power resource, vehicle-to-grid (V2G) is considered as an effective source of flexibility, which is concerned to lack under large amount of VRG. In this study, we analyze the cost reduction effect of using V2G as system flexibility through calculation of day-ahead unit commitment (UC) in Kyushu area. To consider uncertainty of day-ahead UC, we calculate UC simulation with operation reserve requirement considering day-ahead forecast error of photovoltaic generation, followed by economic dispatch simulation using actual photovoltaic generation. V2G as LFC reduces operation cost especially when demand is low, even with 180 000 electric vehicles (EVs). Cost reduction per EV is about 20-80 JPY/day with 180 000 EVs, which saturates if more EV participates in the control. V2G as operation reserve reduces discharge from EV for about 0.5-1.5 kWh/day/EV, which results in reducing degradation of EV battery.

KEYWORDS

economic dispatch control, electric vehicle, system flexibility, unit commitment, variable renewable generation

1 | INTRODUCTION

Renewable energies have been increasingly introduced in the recent years. Thus, the Strategic Energy Plan[1] approved by the Cabinet in July 2018 sets up targets for energy mix in 2030, and stipulates efforts toward renewable energies serving as the main power source. On the other hand, in case of photovoltaic (PV) power generation and wind power generation—called "variable renewable generation" (VRG)—holding a large share in renewable energy introduction, power output depends on weather. It is important to secure regulation capacity to deal with output fluctuations as well as operating reserve to deal with forecast errors (these features are referred below as "system flexibility").

In this context, the Strategic Energy Plan considers, among other measures, the use of vehicle-to-grid (V2G) system that controls reverse power flow from electric vehicles (EVs) and contributes to lower carbon content in regulation capacity. EVs promise not only reduction of greenhouse gas emission in the transportation sector, but also peak-cut and peak-shift due to smart charging (V1G) and V2G; much research and experiments have been conducted in this field. Particularly, Saber et al[2] proposed operation scheduling that presumes securement of operating reserve due to EVs at the moment when unit commitment (UC) is scheduled a day before, and confirmed reduction in committed thermal generators and in operation costs. On the other hand, day-ahead scheduling involves a number of uncertainties including demand forecast, PV output forecast, EV operation, etc. To address these problems, Saber et al[3] analyzed securement of operating reserve by EVs using dynamic programming with regard to uncertainties of EV operation, PV output and wind power output. Besides, Juha et al[4] analyzed operation cost reduction effect of operating reserve securement by EVs with regard to uncertainties; for this purpose, they performed stochastic optimization using probability distribution of wind power output and

power demand. On the other hand, these are hourly analyses using annual travel distance and other data pertaining to EVs. Besides, with the increasing introduction of VRG in Japan, a discussion is held on revision of operating reserve to handle forecast errors. A change in the required amount of operating reserve is thought to alter the role of EVs in power system operation, and analysis of this issue is important in terms of the use of the growing number of EVs.

In this context, the present article estimates EV usage based on the past data and estimates the necessary operating reserve based on the trends in PV forecast errors; in addition, the article evaluates the effect of system operation cost reduction due to system flexibility provided by EVs. In calculation of system operation, we use a UC model that can secure required operating reserve determined based on PV output forecast errors and an economic dispatch control (EDC) model assuming actual operation, with reference to literature.[5,6] Besides, for the purpose of intended evaluation, both models are added with operating reserve due to EV charge/discharge and V2G as well as load frequency control (LFC) coordination. As distinct from stationary battery equipment, EVs are used for customer transportation; therefore, a power system operator can hardly control EV penetration and operation. System flexibility assurance is effective even at a stage of low penetration rate and control participation rate, while increase in the effectivity with higher rates has a strong influence on EV operation in terms of system flexibility. Thus, this article focuses on relationship between flexible system operation and available resources of participating EV batteries to evaluate economic performance of system flexibility assurance with EV control participation rate treated as a parameter.

2 | ESTIMATION OF EV TRAVEL PATTERNS

2.1 | OD data of road traffic census

Trip data (origin-destination data) of 2010 Road Traffic Census are used in this article. First, the vehicles were distributed by type (standard cars and light cars), and then, based on the methodology by Nakaue et al,[7] EVs in Kyushu were classified into 10 groups by the main purpose of use (weekday commuting, weekend commuting, weekday business, weekend business, and recreation). In addition, based on the methodology by Tagashira et al,[8] hourly trip patterns (travel distance, amount of connected EVs) were calculated for each group. Here amount of connected EVs is the number of vehicles parked where charging is possible (in this article: homes, commercial facilities, and places of work). The daily average travel distance is about 15 km. Besides, ad-hoc charging patterns (when EVs with batteries not fully charged perform charging as soon as parked) were generated based on the trip patterns and used as EV charging patterns when V1G or V2G is unavailable.

2.2 | EV penetration rate

In this article, penetration rate is set assuming the profile of the year 2030. Tagashira et al[8] assume EV penetration rate of 30% with reference to the *Options for Energy and Environment* by Energy and Environment Council[9]; the same assumption is adopted in this article. In the Road Traffic Census, one-trip data are used to represent multiple vehicles, and 30% of each trip data are assumed to be substituted by EVs. Passenger car ownership in Kyushu region was 6569, 142 units as per end of March 2010[10]; thus, the number of passenger cars in Kyushu is set to 6 million including 1.8 million of EVs. On the other hand, the number of EVs in Japan per end of financial year (FY) 2016 was about 70 000,[11] which corresponds to about 0.1% in terms of penetration rate.

3 | INTRODUCTION MODELS FOR VARIABLE RENEWABLE GENERATION, OUTPUT FORECAST, AND ACTUAL VALUES

3.1 | Introduction model for PV generation

With reference to the introduction amount of Feed-in Tariff (FIT) system published by the Ministry of Economy, Trade and Industry,[12] FIT system is introduced proportionally in municipalities as per end of FY 2016. In so doing, equipment of 8170 MW (30-day output curtailment limit for FY 2016) is assumed to be introduced in Kyushu.

3.2 | Introduction model for wind power generation and actual output

Introduction ratio is derived for every prefecture based on the introduction potential of onshore wind power published by the Ministry of Environment.[13] Introduction amount for every prefecture is obtained assuming that equipment of 1800 MV (connectable amount for FY 2016) is introduced in Kyushu according to the mentioned introduction ratio.

Actual output is based on hourly wind speed data at observation points corresponding to the seat of every prefectural government, retrieved from the past meteorological data published by the Japan Meteorological Agency.[14] Wind speed is converted into generated output using a wind turbine performance curve (hub height: 60 m, 1000 kW class); wind speed at the hub height is derived using the power law (exponent: 0.5).[15] In Kyushu region, introduction amount of wind power generation is small as compared to PV power generation; thus, forecast errors are ignored in this article for simplicity. In other words, day-ahead forecast values are adopted as actual values.

3.3 | Forecast output and actual output of PV power generation

Forecast data of Numerical Weather Forecasting and Analysis System (NuWFAS) published by the Central Research Institute Electric Power Industry Report[16] are used in calculation of forecast output. The forecast values are set as integrated values of insolation [J/m^2] at each location with time granularity of 30 min and horizontal grid spacing about 4 km. The integrated values are converted into 30-min average instantaneous values (W/m^2), and these are multiplied by PV installed capacity at each grid point and a correction coefficient (0.85) to obtain forecast output. Installed capacity at each grid point is calculated using assigned latitude and longitude, with reference to small region boundary data in the 2015 National Census.[17] Forecasts are updated twice a day, at 9:00 and 21:00; to simulate day-ahead forecast, the forecast data 15-38.5 h ahead of update at 9:00 are used in this article.

Actual output is calculated using the amount of downward solar radiation measured every 2.5 min by the weather satellite Himawari 8 and provided by the Solar Radiation Consortium. Actual values are obtained, same as forecast values, from the data at every hour, horizontal grid spacing being about 1 km. Same as with NuWFAS, latitude and longitude are assigned to every grid point; then the nearest NuWFAS grid points are derived to be applied to municipalities and installed capacity.

3.4 | Forecast accuracy of PV power generation

In this article, forecast error is defined as forecast output value less actual output value, and forecast error rate is defined as the ratio of forecast error to installed capacity. Positive or negative forecast error and forecast error rate mean, respectively, over- or underprediction. Using hourly forecast and actual output data from 00:00 on January 1 through 23:00 on December 31 2016, the 95th percentile of positive and negative forecast error rate was 18.30% and –20.10%, respectively. Forecast error rate is considered only at 6:00-18:00 every day; the other time slots are discarded on the assumption that no PV output is generated. Thus, obtained 95th percentiles are used to derive required reserve.

4 | METHOD OF ANALYSIS

4.1 | Outline

Operation costs are calculated through demand-supply simulations using UC and EDC expressed by mixed integer programming, with reference to literature.[5,6] Simulations deal with day-ahead scheduling and on-the-day operation; at the stage of day-ahead scheduling, reserve must be provided based on PV forecast errors. In this article, economic performance of control methods was evaluated by comparison of results with regard to EV charging/discharging in UC and EDC as well as securement of system flexibility through respective control methods. Unlike in literature,[6] battery storage installed to compensate for LFC coordination is not taken into account. Time granularity is 1 h and time horizon is 2 weeks. The time horizon was set considering that output of VRG varies from day to day, and that pumping operation is scheduled weekly. Two representative weeks are selected in winter season and in midseason to account for seasonal differences in demand and VRG output. In demand-supply adjustment simulations, Kyushu region is geographically approximated by one node, and power transmission and distribution within the node is not considered. Variables used in the following explanations are listed in Table 1. Endogenous variables are denoted by uppercase letters, while exogenous variables, including parameters, are denoted by lowercase letters.

4.2 | Unit commitment scheduling

The objective function in Equation (1) is minimized using PV forecast output, performance of generators and storage facilities, demand load and EV driving pattern as exogenous values. In this expression, the first term is the sum of fuel costs ($a_i{}^{TG}\ P_{t,i}{}^{TG} + b_i{}^{TG}\ U_{t,i}{}^{TG}$) and startup costs ($x_{iTG}\ X_{t,i}{}^{ON}$); the second term is the sum of penalties. The penalties pertain to EV discharging, output curtailment of VRG and insufficient operating reserve. Fuel costs of thermal generators are normally expressed quadratically, but here a linear function is adopted to reduce computational complexity. The penalty coefficient for EV discharging is set to 10/kWh assuming the manufacture cost of 10 000/kWh (battery performance target for 2030[18]) and cycle life of 1000. The penalty coefficient for power curtailment is 5.5/kWh based on the past calculation of average highest fuel price of thermal generators that increase their output during the period of power curtailment. The penalty coefficient for insufficient reserve is set to 192/kWh, that is, 10-fold fuel cost of the most expensive oil-fired power generation. This penalty is imposed to avoid no-solution conditions in optimization calculation.

$$\min \sum_t \sum_i \left(a_i^{TG} P_{t,i}^{TG} + b_i^{TG} U_{t,i}^{TG} + x_i^{TG} X_{t,i}^{ON}\right) + \sum_t \left\{ 5.5 D_t + \sum_c 10 P_{t,c}^{EVD} + 192 \left(INSUF_t^{UP} + \frac{1}{2} INSUF_t^{DN} \right) \right\} \times 10^3. \quad (1)$$

TABLE 1 Variables

t	Time steps
i	Label for generator
j	Label for pumped storage
c	Label for EV groups
$P_{t,i}^{TG}$	Output of generator [MW]
$P_{t,j}^{PMD/PMU}$	Generating/pumping-up output of pumped storage [MW]
$P_{t,c}^{EVD/EVU}$	Discharging/charging output of EV groups [MW]
D_t	VRG curtailment [MW]
$CNG_{t,c}^{EV,UP/DN}$	Upward/downward controllable output of EV groups [MW]
$S_{t,c}^{EV}$	Electricity charged in EV groups [MWh]
$RSV_{t,j}^{PM,UP/DN}$	Upward/downward operating reserve of pumped storage [MW]
$RSV_{t,c}^{EV,UP/DN}$	Upward/downward operating reserve of EV groups [MW]
$LFC_{t,j}^{PMD/PMU}$	LFC of pumped-storage [MW]
$LFC_{t,i}^{EV}$	LFC of EV groups [MW]
$U_{t,i}^{TG}$	On and off state of generator (“0” Off “1” On)
$U_{t,j}^{PMD/PMU}$	On and off state of generating/pumping-up pumped-storage [MW] C “0” Off, “1″ On)
$X_{t,i}^{ON}$	Switching-on signal of generator (“0” No, “1” Yes)
$INSUF_t^{UP/DN}$	Insufficient of upward/downward operating reserve [MW]
$INSUF_t^{P}$	Insufficient power supply [MW]
ed_t	Electricity demand [MW]
$p_t^{PV,F}$	Forecasted output of PV [MW]
p_t^{WIND}	Output of wind generator [MW]
$rsv_t^{req,UP/DN}$	Upward/downward operating reserve requirement [MW]
P_t^{Hydro}	Output of hydro generator [MW]
$p_{MAX,j}^{PMD/PMU}$	Maximum output of generating/pumping-up pumped-storage [MW]
$ev_{t,c}^{ABLE}$	Maximum output of EV groups (amount of connected EVs times 3 MW/1000 EVs) [MW]
$p_{SET,t,c}^{EVU}$	Charging schedule of EV groups at base case [MW]
r_i^{AP}	In-house energy consumption rate of generator [∼]
$lfc_j^{PMD/PMU}$	LFC capacity rate of generating/pumping-up pumped-storage H
$e_{+95th/-95th}^{PV}$	95 percentile of positive/negative forecast error of PV [MW]
x_i^{TG}	Start-up cost of generator [JPY]
a_i^{TG}	Coefficient of fuel cost function [JPY]
b_i^{TG}	Fixed cost of fuel cost function [JPY]
$p_{MAX/MIN,t,c}^{EVU}$	Maximum/minimum charging output of EV groups [MW]
$p_{MAX,t,c}^{EVD}$	Maximum discharging output of EV groups [MW]
$cir^{CHA/DIS}$	Parameter for charging/discharging control (“0” can, “1” cannot)
ctr^{RSV}	Parameter for counting reserve from EV (“0″ can, “1” cannot)
ctr^{LFC}	Parameter for counting LFC from EV (“0” can, “T”cannot)
ctr^{EV}	Participation rate of EVs

Constraints are imposed on demand-supply balance, upper/lower limit of thermal power generation, upper/lower limit of pumping equipment, LFC, GF (Governor Free), operating reserve, pondage, upper/lower limit of thermal operation time, upper/lower limit of EV charging/discharging and EV discharge level (State of Charge: SOC).

The demand-supply balance constraint is shown in Equation (2). Hydro power output is assumed fixed by month based on the actual data of 2004-2013.

$$ed_t = \sum_i^I P_{t,i}^{TG}\left(1 - r_i^{AP}\right) + \sum_j^J \left(P_{t,j}^{PMD} - P_{t,j}^{PMU}\right) + \sum_c^C \left(P_{t,c}^{EVD} - P_{t,c}^{EVU}\right) + p_t^{PV,F} + p_t^{WIND} - D_t + p_t^{Hydro}. \quad (2)$$

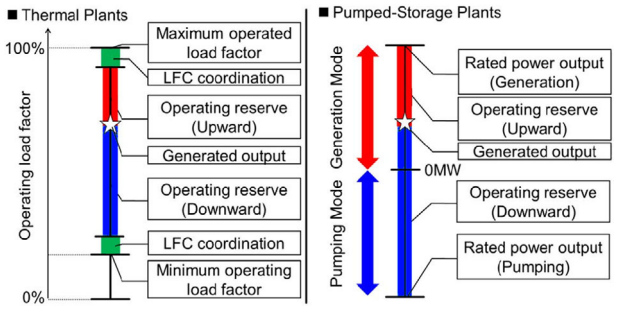

FIGURE 1 Relationship between operating reserve and LFC coordination of thermal and pumped-storage plants [Color figure can be viewed at wileyonlinelibrary.com]

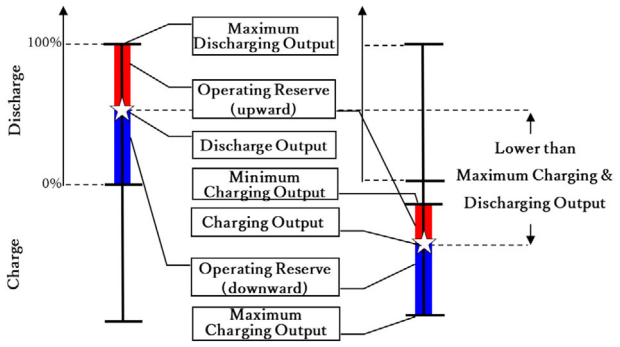

FIGURE 2 Relationship between operating reserve and LFC coordination of EV [Color figure can be viewed at wileyonlinelibrary.com]

As regards possible values of operating load factor for thermal generators and pumps, the values for generators are restricted by constraints on upper/lower limit, LFC, GF, and operating reserve, same as in literature[6] (Figure 1). LFC coordination was assumed at a constant ratio with respect to the rated output of committed generators. Amount of upward/downward operating reserve was defined as the difference between generated output and maximum/minimum output less LFC coordination. Operating reserve provided by pumped storage is available capacity from generated output to maximum output of generators and pump storage, as shown in Figure 1 and Equations (3) and (4). Available amounts of LFC coordination in generation mode and pumping mode in Equations (5) and (6) are determined as the minimum value among upward operating reserve, downward operating reserve, and a certain percentage of rated power output. When the available amount in one mode is positive, the amount in the other mode becomes 0.

Besides, this article assumes two kids of pumping equipment—fixed-speed and variable-speed pumps; in the former case, LFC coordination cannot be provided in pumping mode (${lfc_j}^{PMU} = 0$)

$$RSV_{t,j}^{PM,UP} = p_{MAX,j}^{PMD} - P_{t,j}^{PMD} + P_{t,j}^{PMU}, \tag{3}$$

$$RSV_{t,j}^{PM,DN} = p_{MAX,j}^{PMU} - P_{t,j}^{PMU} + P_{t,j}^{PMD}, \tag{4}$$

$$LFC_{t,j}^{PMD} \le \min\left(p_{MAX,j}^{PMD} lfc_j^{PMD} U_{t,j}^{PMD}, RSV_t^{PM,UP}, RSV_t^{PM,DN}\right), \tag{5}$$

$$LFC_{t,j}^{PMU} \le \min\left(p_{MAX,j}^{PMU} lfc_j^{PMU} U_{t,j}^{PMU}, RSV_t^{PM,UP}, RSV_t^{PM,DN}\right). \tag{6}$$

Upper/lower limit of EV output, LFC coordination and operating reserve are illustrated in Figure 2. The basic approach is same as with pumped storage, but the difference is that charging and discharging can be performed simultaneously when car batteries are treated as an aggregate, and that EVs other than those participating in control follow ad-hoc charging patterns so that a lower limit is imposed on charging power. First, let us explain derivation of minimum and maximum charging output of EV group in Equations (7) and (8). In case that charging control is impossible ($ctr^{CHA} = 0$), only the first term remains in both expressions, and both minimum and maximum charging output of EV group coincides with ad-hoc charging. In case that charging control is possible ($ctr^{CHA} = 1$), only the second term remains in both expressions, and minimum/maximum charging outputs correspond to control participation rate. Among vehicles connected to the grid, those not participating in control follow ad-hoc charging, while charging output of the vehicles participating in control is 3 kW per vehicle at maximum and 0 kW per vehicle at minimum. Similarly, Equation (9) pertains to derivation of maximum discharging output of EV group. In case that discharging control is impossible ($ctr^{DIS} = 0$), the maximum value is 0; in case that discharging control is possible ($ctr^{DIS} = 1$), the maximum value is 3 kW per vehicle for EVs connected to grid and participating in control. Next Equations (10) and (11) show upward/downward operating reserve provided by EVs. Only when operating reserve by EVs is possible ($ctr^{RSV} = 1$), reserve can be provided according to possible output variation range. The possible output variation range is defined as a margin from EV charging/discharging output to maximum and minimum output as shown in Equations (12) and (13). There are two direction of possible output variation range; the upward direction corresponds to increase in power supply, and the downward direction corresponds to increase in demand load. Finally, derivation of LFC coordination by EVs LFC_t^{EV} is shown in Equation (14). Only when LFC coordination by EVs is possible ($ctr^{LFC} = 1$), LFC coordination is provided according to upward or downward EV possible output variation range, whichever is smaller.

$$p_{MAXt,c}^{EVU} = (1 - ctr^{CHA}) p_{SETt,c}^{EVU} + ctr^{CHA}\left\{p_{SETt,c}^{EVU}(1 - ctr^{EV}) + ctr^{EV} ev_{t,c}^{ABLE}\right\}, \tag{7}$$

$$p^{EVU}_{MINt,c} = (1 - ctr^{CHA})\, p^{EVU}_{SETt,c} + ctr^{CHA} \left\{ p^{EVU}_{SETt,c} (1 - ctr^{EV}) \right\}, \tag{8}$$

$$p^{EVD}_{MAXt,c} = ctr^{DIS} ctr^{EV} ev^{ABLE}_{t,c}, \tag{9}$$

$$RSV^{EV,UP}_{t,c} \leq ctr^{RSV}\, CNG^{EV,UP}_{t,c}, \tag{10}$$

$$RSV^{EV,DN}_{t,c} \leq ctr^{RSV}\, CNG^{EV,DN}_{t,c}, \tag{11}$$

$$CNG^{EV,UP}_{t,c} = p^{EVD}_{MAXt,c} - P^{EVD}_{t,c} + P^{EVU}_{t,c} - p^{EVU}_{MINt,cc}, \tag{12}$$

$$CNG^{EV,DN}_{t,c} = p^{EVU}_{MAXt,c} - P^{EVU}_{t,c} + P^{EVD}_{t,c}, \tag{13}$$

$$LFC^{EV}_{t,c} \leq ctr^{LFC} \times \min \left(CNG^{EV,UP}_{t,c}, CNG^{EV,DN}_{t,c} \right). \tag{14}$$

LFC coordination is restricted so that its total reserve provided by thermal generators, pumped storage, and EVs is no less than 3% of daily maximum demand. GF equivalent is restricted so that total reserve of LFC coordination by thermal generators and pumped storage is no less than power demand at each time point, while provision due to EVs is not recognized. Operating reserve is restricted so that its total amount provided by thermal generators, pumped storage, and EVs is no less than the required amount in Equation (15).[6] This required operating reserve is the square root of the sum of squares of 3% power demand and 95th percentile of PV forecast error. Since PV power is not generated in night hours, required operating reserve at 19:00 through 5:00 next day is simply 3% power demand.

$$rsv^{req,UP/DN}_{t} = \sqrt{\left(0.03 ed_t\right)^2 + e^{PV}_{+95th/-95th^2}}. \tag{15}$$

With the pondage constraint, water storage rate in the morning of Monday is set to 50%. In addition, to avoid supply deficit in real operation, the minimum pondage (3540 MWh) is obtained so that rated output of the most powerful unit (Unit 3 of Genkai Nuclear Power Plant: 1180 MW) can be maintained for 4 h.[19] As regards constraint on operation time of thermal generators, minimum continuous start time and minimum continuous stop time are set for each thermal generator. Besides, constraint on pumped-storage generation mode requires that pumps may not operate in generation mode and pumping mode simultaneously. To make allowance for scheduled inspection of nuclear and thermal power plants in constraint on utilization factor, based on the maximum monthly demand in 2016, the factor is set to 90% during 4 months of the highest demand, 70% during 4 months of the lowest demand, and 80% during the remaining 4 months.[20] As regards EV battery storage, three types of constraints are imposed: on upper/lower limit of storage, on storage at departure, and on temporal energy conservation. The upper limit of storage was set to 24 kWh per vehicle for standard cars and 16 kWh per vehicle for light cars; the lower limit was set to 30% for both types.[21] Besides, the storage at departure was restricted so that the state of charge was 80% or higher at 6:00 every morning.[21] Temporal energy conservation is formulated in Equation (16). Here charge-discharge efficiency is set to 95% one way.

$$S_{t+1,c} = S_{t,c} - P^{EVD}_{t,c}/0.95 + 0.95 P^{EVU}_{t,c} - Drive_{t,c}. \tag{16}$$

5 | ECONOMIC DISPATCH CONTROL

The objective function in Equation (17) is minimized using actual PV output, UC schedule, performance of generators and storage facilities, demand load and EV driving pattern as exogenous values. The first and second terms of the expression pertain to the total fuel costs and penalties, respectively. The penalties pertain to EV discharging, output curtailment of VRG, and insufficient operating reserve. The penalty is imposed to avoid no-solution conditions in optimization calculation; to prevent supply deficit due to cost reduction, the penalty coefficient set to 192/kWh, that is, 10-fold fuel cost of the most expensive oil-fired power generation.

$$\min \sum_{t}^{T} \sum_{i}^{I} \left(a^{TG}_{i} P^{TG}_{t,i} + b^{TG}_{i} U^{TG}_{t,i} \right) + \sum_{t}^{T} \left\{ 5.5 D_t + \sum_{c}^{C} 10 P^{EVD}_{t,c} + 192\, INSUF^{p}_{t} \right\} \times 10^3. \tag{17}$$

Constraints are imposed on demand-supply balance, upper/lower limit of thermal power generation, upper/lower limit of pumping equipment, LFC, GF, operating reserve, pondage, generation mode of pumped storage, upper/lower limit of EV charging/discharging and EV storage. Required amount of reserve is set to no less than 3% power demand at each time point; requirements for LFC coordination and GF are set same as with UC. In addition, in case that operating reserve can be provided by EVs, EV charging/discharging schedule can be varied within the limit power range determined by Equations (10)-(12). In case that operating reserve cannot be provided, amount of charging/discharging in EDC follows the schedule determined with UC.

TABLE 2 Case statements according to purpose of V2G (set for LFC cases)

	Base	V1G	V2G	V1G-LFC	V2G-LFC
UC	No Charging/discharging control	Leveling net load (charging only)	Leveling net load	Leveling net load + LFC securing (Charging Only)	Leveling net load + LFC securing
EDC	Following schedule at UC				

TABLE 3 Case statements according to purpose of V2G (set for RSV cases)

	Base	V2G	V2G-RSV
UC	No charging/discharging control	Leveling net load	Leveling net load + Operating reserve securing
EDC	Following schedule at UC		Leveling net load

5.1 | Analysis conditions

Base on power demand magnitude, two representative weeks are selected in winter season and in midseason as analysis periods. In addition to weekly operation schedule of pumping equipment, biweekly calculation period was set for greater generality. Time series data of January 15-28 and April 20-May 13 were used for the representative weeks. Hydro power output is 314.2 and 487.0 MW, respectively. Thermal generators were 32 real plants in Kyushu region including four types fueled by coal, LNG (liquefied natural gas), LNGCC (LNG combined cycle), and oil. Fuel grades and rated output of thermal power plants were set with reference to literature.[22] The upper limit of equipment utilization factor is 90% in winter season and 70% in midseason. Two types of pumping equipment were included in the model—fixed-speed pumps of 1100 MW and variable-speed pumps of 1200 MW. Several cases listed in Tables 2 and 3 were considered depending on the purpose of EV charge/discharge control. The number of EVs participating in control was set to 180 000, 270 000, 360 000, 450 000, 540 000, and 900 000 out of a total of 1.8 million vehicles. The vehicles participating in control are controller by the listed cases, while the rest of the vehicles are assumed to follow ad-hoc charging. The ratio of the participating EVs to the total is 10%-50%. The maximum charging/discharging output per EV is set to 3 kW.

6 | RESULTS OF ANALYSIS

Operation costs defined as the sum of UC startup costs and EDC fuel costs are used as an index of economic performance. In this article, convergence test error in optimization calculation is set to 0.15%.

6.1 | Winter season

Figure 3 shows operation costs obtained through calculation of 36 combinations of control purpose and participation, and normalized with respect to the operation cost of base case with

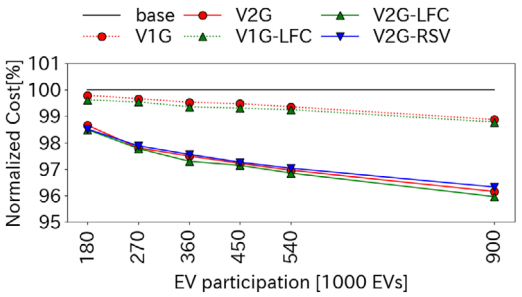

FIGURE 3 Normalized operation costs in winter [Color figure can be viewed at wileyonlinelibrary.com]

180 000 vehicles participating in control (14-day startup costs of 490 million yen + fuel costs of 17.49 billion yen = 17.98 billion yen). As can be seen from the diagram, there is no significant difference in operation costs between control cases aimed at securement of system flexibility (V1G-LFC, V2G-LFC, V2G-RSV) and those aimed only at net load leveling (V1G, V2G). For more detailed analysis, representative weeks of winter season are divided into high-demand days and low-demand days.[1] Normalized operation costs for high- and low-demand days are shown in Figure 4 (the base case corresponds to 59.0% and 41.0%, respectively). On high-demand days, there is no substantial difference between control aimed only at net load leveling and control providing system flexibility, same as in Figure 3. On the other hand, on low-demand days, the cases V1G-LFC and V2G-LFC providing LFC coordination offer reduction of operation costs up to 0.5% as compared to the cases V1G and V2G aimed only at net load leveling.

Here, we explain how EV-based LFC capacity affects operation of thermal generators and pumping equipment. Figure 5 shows available LFC power reserve during 2 days (high-demand day of January 15 and low-demand day of January 16) in the cases V1G and V1G-LFC, V2G and V2G-LFC, with participation of 540 000 vehicles. In the case

[1] Daily analysis of operation costs revealed certain trends corresponding to demand magnitude; thus, daily demand curves are used in clustering by Ward's method. High-demand days are the 7 days of January 15 and 22-28, and the rest are low-demand days.

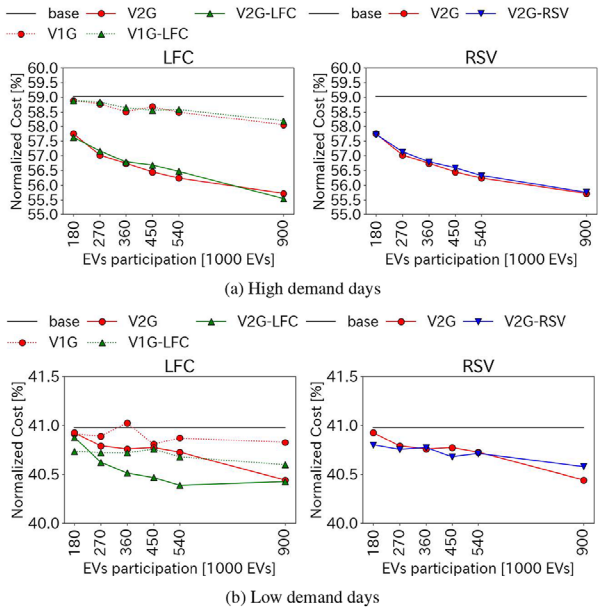

FIGURE 4 Normalized operation costs on high-demand days and low-demand days in winter [Color figure can be viewed at wileyonlinelibrary.com]

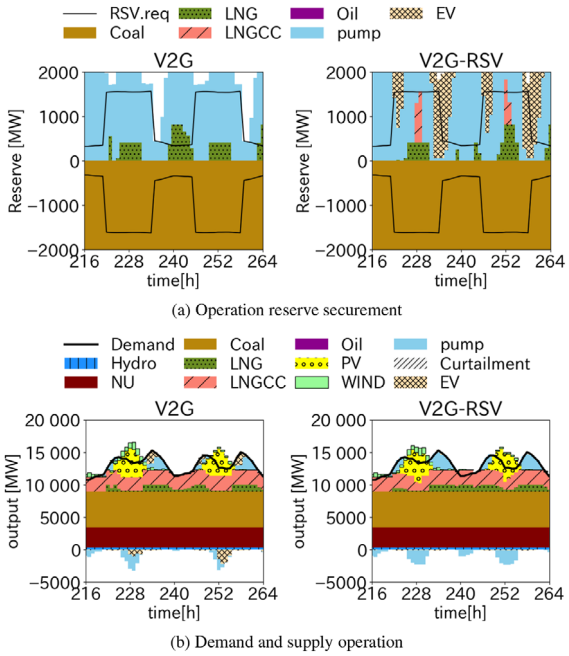

FIGURE 6 Operation with 900 000 EVs on January 24-25 [Color figure can be viewed at wileyonlinelibrary.com]

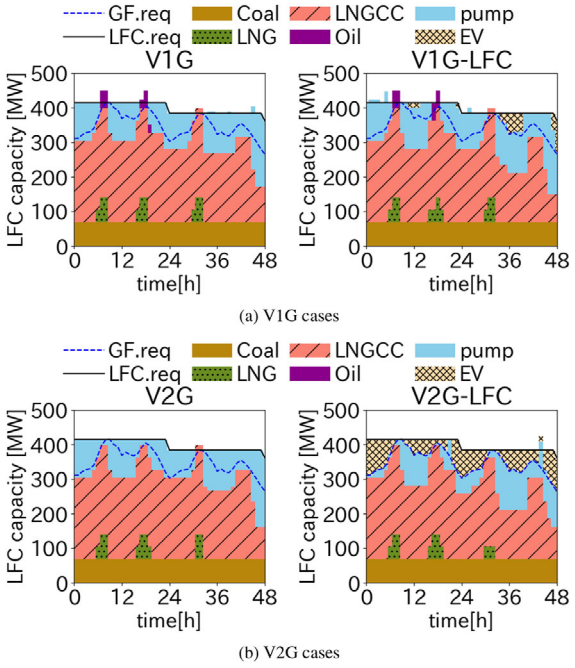

FIGURE 5 LFC securement with 540 000 EVs on January 15-16 [Color figure can be viewed at wileyonlinelibrary.com]

V1G-LFC when LFC coordination is provided only through charging control, LFC capacity can be only secured during EV charging. Therefore, LFC capacity by EVs is only secured either in nighttime when power demand is low or in daytime when PV output is high. Besides, EV charging is performed on low-demand days when power demand is low; therefore, available LFC capacity is smaller on high-demand days. The diagram also confirms that in the V1G-LFC case, commitment of thermal generators is reduced according to required LFC capacity by EVs, and one can conclude that operation costs on low-demand days are reduced due to lower fuel costs. In the V2G-LFC case, LFC capacity can be secured as long as controllable EVs are available, even without charging; thus, EV-based LFC coordination can be confirmed throughout the day. On the other hand, LFC capacity provided by thermal generators is reduced throughout the day on low-demand days, but only in daytime on high-demand days. This can be explained by the fact that on high-demand days, thermal power generation is needed to meet power demand and to provide required reserve even though EVs take over that task of providing LFC capacity. Thus, the number of committed thermal generators cannot be reduced, which can explain the fact that operation costs on the high-demand day were not cut as compared to the V2G case. LFC capacity provided by EVs is up to 117 MW in the case of V1G-LFC and up to 132 MW in the case of V2G-LFC, which corresponds to participation about 40 000 vehicles. This result suggests that even a small number of participating EVs may contribute to LFC coordination.

Next, let consider how EV-based operating reserve affects operation of thermal generators and pumping equipment. As can be seen in Figure 4, operating reserve provided by EVs has hardly any effect on operation cost reduction in winter season, but EV discharge decreases. Figure 6 illustrates operating reserve securement and demand-supply operation during 2 days (January 24 and 25, both are high-demand days) in the cases V2G and V2G-RSV with participation of 900 000

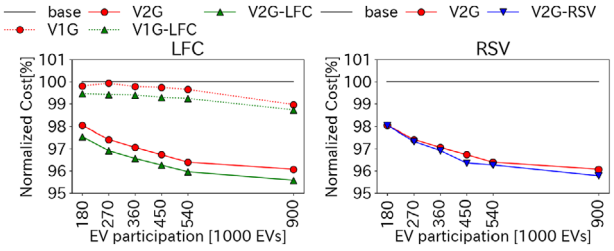

FIGURE 7 Normalized operation costs in spring [Color figure can be viewed at wileyonlinelibrary.com]

EVs. In the case V2G-RSV, upward operating reserve provided by EVs substitutes reserve of pumps and LNG plants in morning and evening hours of high demand. Such substitution contributes to reduction of committed thermal generators during those time slots; moreover, generated output of pumped storage is no longer needed for upward operating reserve, and used instead of EV discharging that occurred in the case V2G. This decrease in EV discharge corresponds to 1.5 kWh/day per participating vehicle, which is important in terms of preventing deterioration of EV batteries. The value of 1.5 kWh is close to energy needed for daily travel distance of 15 km in the driving pattern assumed in this study. On the other hand, as can be also seen in Figure 4, operation cost reduction in the case V2G-RSV against V2G is within the limits of error. The fact that operation costs are not reduced though less thermal power plants are committed during morning and evening hours is explained by increase in thermal plant commitment during daytime. One can think that startup costs and fuel costs increased because thermal generators compensated for LFC capacity that could not be provided by fixed-speed pumps operating in pumping mode during daytime. Now, contribution to upward operating reserve is confirmed beginning from 180 000 participating EVs.

6.2 | Midseason

Similar to winter season, Figure 7 shows operation costs normalized with respect to the operation cost of base case with 180 000 vehicles participating in control (14-day startup costs of 320 million yen + fuel costs of 7.64 billion yen = 7.96 billion yen). As distinct from winter season, clustering by load curves was not performed in midseason. Besides, the effect of LFC coordination is similar to that confirmed on low-demand days of winter season, thus, being omitted here.

Figure 8 illustrates operating reserve securement and demand-supply operation during 2 days (May 4 and 5) in the cases V2G and V2G-RSV with participation of 900 000 EVs. Unlike in winter season, downward operating reserve by EVs was confirmed in midseason. In the case V2G, downward operating reserve that was provided by pumping was substituted by EVs; as a result, pumping output increased, and pumps replaced EV discharging in daytime bottom-

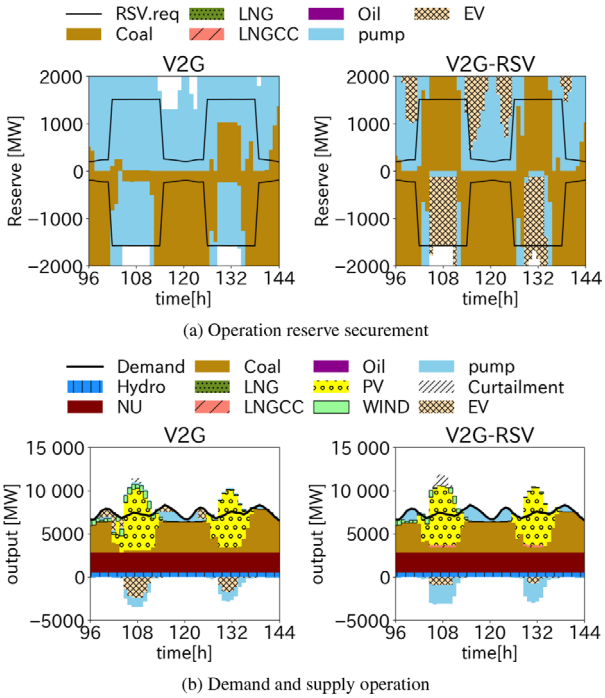

FIGURE 8 Operation with 900 000 EVs on May 4-5 [Color figure can be viewed at wileyonlinelibrary.com]

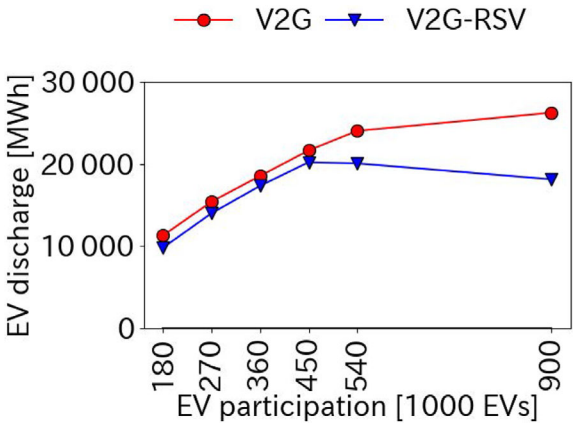

FIGURE 9 EV discharge in spring [Color figure can be viewed at wileyonlinelibrary.com]

up operations and demand-supply balancing. The daytime bottom-up operations are confirmed beginning from 180 000 participating EVs, but substitution of pumping with EV discharging is confirmed only with 540 000 or more EVs. However, more LNGCC plants are committed to compensate for LFC capacity deficient because of pumping operation of fixed-speed pumps, which brings about increase of fuel costs, and operation costs are hardly reduced as compared to the case V2G. On the other hand, as can be seen from EV discharge in every case shown in Figure 9, the difference in discharge between V2G and V2G-RSV remains unchanged with EV participation up to 450 000 vehicles. When 540 000 and more vehicles participate in control, decrease in EV discharge due

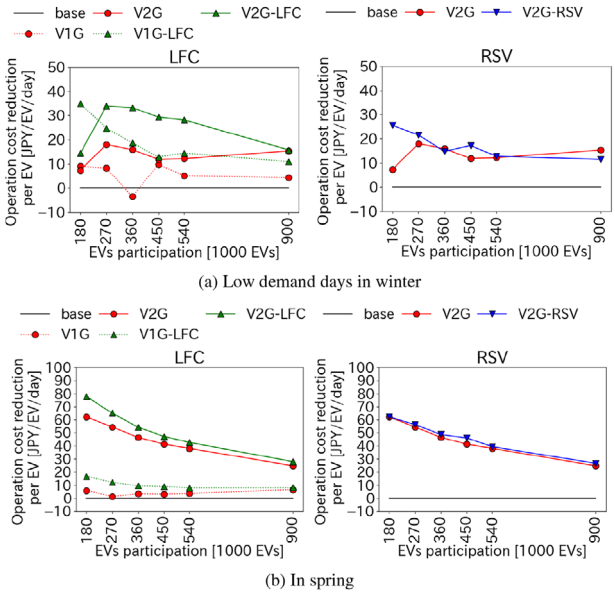

FIGURE 10 Cost reduction per EV [Color figure can be viewed at wileyonlinelibrary.com]

to operating reserve securement grows to 0.5 kWh/day in per-vehicle terms. In addition, output curtailment of about 35 GWh (about 5.9%) occurs in the base case; in contrast, output curtailment rate is reduced to 0% with participation of 900 000 EVs in the most efficient case of V2G-RSV. From the above, one may conclude that operating reserve securement by V2G has a small effect on reduction of operation costs, but a great effect on reduction of output curtailment and EV discharge.

6.3 | Reduction of per-vehicle operation cost

This subsection considers reduction of operation cost per participating vehicle with respect to the base case. Figure 10 shows the difference between base case and each case, divided by the number of participating EVs and the number of days. From these results, one can derive the upper limit of incentives paid by system operators for 1-day EV participation in each control case. Comparison is based on the assumptions that electricity about 1.5 kWh is consumed by one EV that travels 15 km a day, and that cost about 30 yen is required to charge the corresponding energy.

On the low-demand days in winter, the maximum per-vehicle daily operation cost reduction in the case V1G-LFC is 35 yen with participation of 180 000 EVs, and then saturates as more EVs are involved in control. In the V2G-LFC case, per-vehicle daily operation cost reduction reaches its maximum of 33 yen with 270 000 EVs, and then also saturates with more EVs. Operation cost reduction in the case V2G-RSV is 10-20 yen/vehicle/day, nearly same as in V2G.

In midseason, operation cost reduction in both cases V1G-LFC and V2G-LFC is the highest with 180 000 EVs, reaching 17 yen/vehicle/day and 78 yen/vehicle/day, respectively. Same as in winter season, cost reduction saturates as EV participation grows, being 8 yen/vehicle/day and 30 yen/vehicle/day, respectively, with 900 000 vehicles. The case V2G-RSV is not much different from V2G; the cost reduction is 62 yen/vehicle/day with 180 000 EVs, and then tends to saturate with participation.

7 | CONCLUSIONS

Assuming EV driving patterns based on past data for passenger cars, this article used a UC-EDC model of power reserve securement with regard to forecast errors of PV output to evaluate how providing system flexibility through EV charging/discharging control affects economic performance, depending on control participation. Providing LFC capacity by means of EVs is expected to reduce operation costs even with a small EV participation when demand is low, and incentives granted to EV owners were confirmed to exceed electricity cost for a daily trip. It was also shown that with operating reserve provided by EVs, amount of EV discharge can be reduced by about 1.5 kWh/vehicle/day due to securement of upward operating reserve in morning and evening hours of winter season; on the other hand, downward operating reserve in daytime of midseason contributes to bottom-up operations as well as reduction of EV discharge and output curtailment. In addition, in case of downward operating reserve securement, output curtailment rate of about 5.9% in the base case was reduced to 0% due to participation of 900 000 EVs.

Topics for future study include consideration of PV output in terms of required LFC capacity. In addition, representative weeks were selected with regard to magnitude of power demand in this study, but it would be important to increase generality by considering weeks with big forecast errors, or by extending the calculation period.

ACKNOWLEDGMENT

We express our gratitude to the Solar Radiation Consortium for providing us with solar radiation data observed by Himawari 8.

REFERENCES

1. Ministry of Economy, Trade and Industry. Strategic energy plan, 2018. (in Japanese)
2. Saber AY, Venayagamoorthy GK. Intelligent unit commitment with vehicle-to-grid —a cost-emission optimization. *J Power Sources*. 2010;195:898-911.
3. Saber AY, Venayagamoorthy GK. Resource scheduling under uncertainty in a smart grid with renewables and plug-in vehicles. *IEEE Syst J*. 2012;6:103-109.

4. Juha K, Peter M. Methodology for modelling plug-in electric vehicle in the power system and cost estimates for a system either smart or dumb electric vehicles. *Energy* 2010;36(3):1758-1767.
5. Udagawa Y, Ogimoto K, da Silva JG, Ohtake H, Fukutome S. Economic impact of photovoltaic power forecast error on power system operation in Japan. IEEE Power Tech, Conference paper, Manchester, UK, 2017.
6. Izumida Y, Asano H, Bando S. Economic analysis of operating reserve using forecasted variable renewable generation. *IEEJ Trans PE*. 2018;138(9):757-765. (in Japanese)
7. Nakaue S, Yamamoto H, Yamaji K, et al. Evaluation of penetration of plug-in hybrid electric vehicles and CO_2 emissions considering utilization patterns and power generation mix. *J Jpn Inst Energy*. 2010;89:249-258. (in Japanese)
8. Tagashira N, Takagi M. An estimation of electric vehicle load profiles in service areas of ten electric power companies in Japan. Central Research Institute Electric Power Industry Report, Y13009, 2014. (in Japanese)
9. Energy and Environment Council. Options for energy and environment, 2012. (in Japanese)
10. Automobile Inspection and Registration Association. Total car ownership. https://www.airia.or.jp/publish/statistics/number.html. Accessed 12 February 2019. (in Japanese)
11. Next Generation Vehicle Promotion Center. EV ownership statistics. http://www.cev-pc.or.jp/tokei/hanbai.html. Accessed 12 February 2019. (in Japanese)
12. Ministry of Economy, Trade and Industry. Feed-in tariff system website. http://www.enecho.meti.go.jp/category/saving_and_new/saiene/statistics/past.html. Accessed 12 February 2019. (in Japanese)
13. Ministry of Environment. Survey report on renewable energy introduction potential in FY 2010, 2011. (in Japanese)
14. Japan Meteorological Agency. Past meteorological data download. https://www.data.jma.go.jp/gmd/risk/obsdl/index.php. Accessed 18 October 2018. (in Japanese)
15. New Energy and Industrial Technology Development Organization. Report on wind power generation field test in Otokoro, Beppu City, 2004. (in Japanese)
16. Hashimoto A, Hirakuchi H. Enhancement and accuracy evaluation of Numerical Weather Forecasting and Analysis System (NuWFAS) for the Hokkaido Island. Central Research Institute Electric Power Industry Report, N09024, 2010. (in Japanese)
17. Ministry of Internal Affairs and Communications. Portal site of official statistics in Japan "e-Stat": statistics map of Japan (Statistics GIS). https://www.e-stat.go.jp/gis. Accessed 18 October 2018. (in Japanese)
18. New Energy and Industrial Technology Development Organization. NEDO Battery RM2013, 2013. (in Japanese)
19. Kyushu Electric Power Co., Inc. Connectable capacity of renewable energy (output of FY 2017), 2017. (in Japanese)
20. Nagai Y, Yamamoto H, Okada K, Yabe K, Nagata Y. Development of a power generation optimization model with bilateral poser intertrade. Central Research Institute Electric Power Industry Report, Y15021, 2016. (in Japanese)
21. Oda T, Maekawa T, Watanabe Y, Aziz M, Kashiwagi T. Questionnaire survey results of charging necessity for electric vehicle users. Proceedings of the 34th Conference on Energy, Economy, and Environment, 2018:591-596. (in Japanese)
22. Electricity and Gas Industry Department, Agency for Natural Resources and Energy, Ministry of Economy, Trade and Industry. Outline of electric power development 2010, 2012. (in Japanese)

AUTHOR BIOGRAPHIES

Nanami Yoshioka is a member. In 2019, she completed master's course at the University of Tokyo (Grad. School of Frontier Sci.). She conducted her research in demand-supply operation. Currently, she is a researcher at Central Research Institute of Electric Power Industry. She has done Masters in Environmental Science.

Hiroshi Asano is a senior member. In 1984, he completed master's course at the University of Tokyo. He first becomes Assistant professor, then professor at the University of Tokyo, and then, he is presently associate vice president, the Central Research Institute of Electric Power Industry, professor, Gifu University, visiting professor, the University of Tokyo, and professor, Tokyo Institute of Technology. He conducted his research in analysis and evaluation of energy systems. He completed his doctorate in Engineering. He is also a JSER President. He is the member of the following groups: IEEE, CIGRE, and IEEE.

Shigeru Bando is a member. In 2005, he completed his doctorate at the University of Tokyo (Grad. School of Frontier Sci.). He was a lecturer at the University of Tokyo (Grad. School of Eng., Dept. of Mech. Eng.), and he is now a senior research scientist of Central Research Institute of Electric Power Industry. Also, he is a visiting associate professor at the University of Tokyo (Grad. School of Frontier Sci.). He conducted his research in energy system analysis with focus on smart grids and demand response. He completed his doctorate in Environmental Science of the University of Tokyo.

How to cite this article: Yoshioka N, Asano H, Bando S. Economic evaluation of charging/discharging control of electric vehicles as system flexibility considering control participation rate. *Electr Eng Jpn*. 2020;211:15–25. https://doi.org/10.1002/eej.23267